
(This is a sample cover image for this issue. The actual cover is not yet available at this time.)

Spectrochimica Acta Part A: Molecular and Biomolecular Spectroscopy 97 (2012) 111–118

Contents lists available at SciVerse ScienceDirect

Spectrochimica Acta Part A: Molecular and Biomolecular Spectroscopy

journal homepage: www.elsevier.com/locate/saa

# Variational study on the vibrational level structure and vibrational level mixing of highly vibrationally excited $S_0$ $D_2CO$

Svetoslav Rashev [a,*], David C. Moule [b], Vladimir Rashev [c]

[a] Institute of Solid State Physics, Bulgarian Academy of Sciences, Tsarigradsko chaussee 72, 1784 Sofia, Bulgaria
[b] Department of Chemistry, Brock University, St. Catharines, ON, Canada L2S3A1
[c] Balkan Services Ltd., 31 Exarch Joseph str., 1000 Sofia, Bulgaria

## HIGHLIGHTS

- We perform large scale converged variational vibrational calculations on $S_0$ $D_2CO$.
- Calculated frequencies are compared to existing experimental data.
- We study the spectral structure and IVR dynamics at very high excitation energy.

## GRAPHICAL ABSTRACT

Calculated spectrum of a highly excited overtone state in $S_0$ $D_2CO$.

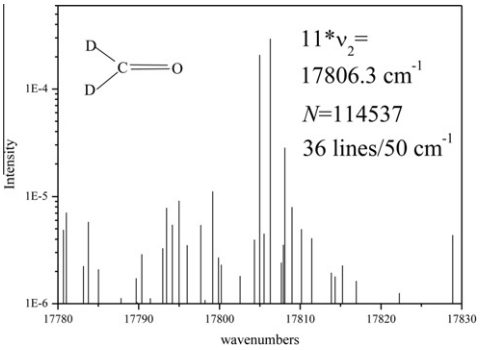


## ARTICLE INFO

*Article history:*
Received 27 February 2012
Received in revised form 22 May 2012
Accepted 26 May 2012
Available online 7 June 2012

## ABSTRACT

We perform converged high precision variational calculations to determine the frequencies of a large number of vibrational levels in $S_0$ $D_2CO$, extending from low to very high excess vibrational energies. For the calculations we use our specific vibrational method (recently employed for studies on $H_2CO$), consisting of a combination of a search/selection algorithm and a Lanczos iteration procedure. Using the same method we perform large scale converged calculations on the vibrational level spectral structure and fragmentation at selected highly excited overtone states, up to excess vibrational energies of $\sim$17000 $cm^{-1}$, in order to study the characteristics of intramolecular vibrational redistribution (IVR), vibrational level density and mode selectivity.



## Introduction

Formaldehyde $H_2CO$ is one of the most popular polyatomics, whose ground electronic state $S_0$ vibrational structure has been studied spectroscopically up to quite high excess vibrational energies ($E_v$) [1–7]. The exact vibrational kinetic energy operator (KE) of formaldehyde was first derived by Handy already in 1987 [8]. For this reason and others formaldehyde has served for many years as a testing ground for many variational, perturbative and algebraic methods for vibrational calculations [9–23], that were also aimed at deriving a precise and reliable potential energy surface (PES) [9,14,16,23].

Recently we developed a specific vibrational variational calculation method [24,25], that was based on the exact KE expression [8] and a PES which had to be presented in separable (factorized) form. In a first application of this method to formaldehyde $H_2CO$ [25], using the realistic (albeit not spectroscopically correct) Martin, Lee, Taylor (MLT) quartic PES [26], we were able to perform converged high precision calculations on the vibrational level

* Corresponding author. Fax: +359 2 975 36 32.
*E-mail address:* rashev@issp.bas.bg (S. Rashev).

1386-1425/$ - see front matter © 2012 Elsevier B.V. All rights reserved.
http://dx.doi.org/10.1016/j.saa.2012.05.056

structure and IVR behavior of a large number of vibrational levels, including highly excited overtone levels at energies up to $E_v \sim 17000\ cm^{-1}$, where the vibrational level density is quite high.

Formaldehyde $D_2CO$ has the same PES as $H_2CO$ (within the Born–Oppenheimer approximation), but a substantially different KE operator, in which the H mass is replaced by D. In contrast to $H_2CO$, for $S_0$ $D_2CO$ few experimentally measured frequencies are available in the lower $E_v$ range [2,27–29]. However this situation is reversed at the very high $E_v \sim 28300\ cm^{-1}$ (close to dissociation threshold). Indeed, using Stark level crossing spectroscopy, Polik et al. [30] have been able to register the $D_2CO$ $S_0$ vibrational level structure in this energy range, whose density was found to exceed by a factor of six the expected value, estimated using standard level counting techniques. (While the single vibrational levels of $H_2CO$ in this energy range could not be resolved, and their density not estimated, probably due to their large and overlapping dissociative widths [30]). This observation raised serious questions, since the vibrational level density is known to be an important factor in the interesting photophysical and photochemical behavior of $D_2CO$ – namely IVR, monomolecular dissociation $D_2CO \rightarrow D_2 + CO$ and intersystem crossing (ISC) $T_1 \rightarrow S_0$ in this energy range, which was found to be quite different from that of $H_2CO$ [30–32].

Concentrating on the IVR issue it must be noted, that this observed density is the vibrationally coupled density, which may be only part of the entire available density, if IVR is not complete in this energy range. Indeed, it has been demonstrated for a number of molecules, that IVR may be restricted and well isolated bright (edge) states may exist up to very high $E_v$ (and even above the dissociation limit) [33–36].

Since both molecules have essentially the same PES (disregarding nonadiabatic coupling effects), all differences in their photophysical and photochemical behavior should be almost entirely due to the different masses in their KE operators. In this respect it may be interesting and instructive to study the vibrational structure and IVR character of vibrationally excited feature states in $D_2CO$, as high as possible in $E_v$, and to compare them with the $H_2CO$ results, obtained in our recent work [25], using the same PES of MLT[26]. Our vibrational method is suitable for such studies because it yields both the dilution factor $\sigma$ [37] as well as the vibrationally coupled level density at the selected highly excited feature states, that are both useful monitors for the extent of vibrational fragmentation and IVR. Recently, Pasin et al., using the Davidson and Multi configuration time dependent Hartree (MCTDH) algorithms, have studied vibrational structure and IVR behavior in highly vibrationally excited HFCO [38] and DFCO [39], and found them to be substantially different.

Our aim in this work is twofold: first, we calculate exact frequencies for a large number of $S_0$ $D_2CO$ vibrational levels in the lower range of $E_v$ (up to $\sim 4500\ cm^{-1}$) and compare our results with the existing experimentally measured values as well as with calculations by other authors. These extensive data may be useful for assignments of future experimental spectroscopic measurements. Second, we present the results from our converged calculations on some very highly excited overtone levels of the $\nu_2$(C-O stretch) and $\nu_4$(out-of-plane bend) modes, in order to study (and compare) their spectral structure as well as the surrounding vibrational level densities, as an indication of their IVR characteristics. We note that the converged vibrational calculations at the higher $E_v$ in $D_2CO$ are a greater challenge than for $H_2CO$, since the vibrational level density in $D_2CO$ grows more steeply with $E_v$ (because of the lower fundamental frequencies).

This work is organized as follows. In section 'Vibrational Hamiltonian, basis set functions, search/selection procedure and Lanczos iteration' we give a brief description of the technical features of our method (vibrational coordinates and Hamiltonian, vibrational basis set, search/selection algorithm and Lanczos iteration), that has been described in greater detail in our recent work on formaldehyde $H_2CO$ [25]. Next, in section 'Vibrational calculations' we describe the results from our calculations on a large number of $D_2CO$ vibrational levels, in the range up to $E_v \sim 4500\ cm^{-1}$. We also present and discuss the results from our large scale calculations on the vibrational structure and IVR characteristics of highly excited $\nu_2$ and $\nu_4$ overtone states up to $E_v \sim 17000\ cm^{-1}$ and compare them with our recent results on $H_2CO$. section 'Conclusions' contains our conclusions from the results of the calculations.

## Vibrational Hamiltonian, basis set functions, search/selection procedure and Lanczos iteration

For the KE of $D_2CO$ we use the expression of Handy [8], in terms of his curvilinear coordinates $q_k$ (three bond stretches, two interbond angles and one dihedral "book" angle). Next for the PES of $S_0$ formaldehyde, we use the original ab initio MLT quartic field [26]. Despite the fact, that this surface does not give spectroscopic accuracy, we have chosen to work with it (at this stage) because it is both realistic and very suitable for our vibrational method, allowing the calculations to access very high $E_v$, where IVR may be explored.

Our 6D basis functions are products of 6 1D basis functions, $\Psi_i = \prod \chi_{n_k}(q_k)$. Alternatively in state space, we denote the basis functions as $|n_1,n_2,n_3,n_4,n_5,n_6; S\rangle$, where $S$ is the symmetry species (we work with symmetrized $\Psi_i$ functions). Our basis functions are chosen to resemble most closely the lower excited molecular vibrational eigenfunctions so that the nondiagonal Hamiltonian matrix elements be as small as possible. For the three stretching coordinates of the C–$D_1$, C–$D_2$ and C–O bonds, we employ Morse oscillator eigenfunctions $\chi_{n_k}(q_k)$, $k = 1,2,3$ $n_k = 0,1,\ldots, n_{k0}$ that are optimally adapted to the relevant molecular motions, by setting appropriately the two parameter values of the Morse oscillators. For the out of plane bend, we employ harmonic oscillator eigenfunctions $\chi_{n_4}(q_4)$ [$q_4 = \phi$ – the out-of-plane bend ("book") angle]. Finally, for the two O–C–D($\theta$) bends (coordinates $q_5 = \cos\theta_1$, $q_6 = \cos\theta_2$), we use a set of normalized associated Legendre polynomials , $n = 2,3,\ldots$, that cancel the singularities in the KE operator. However, since they have no free parameters to adjust and are not well adapted to the molecular vibrations, for them we apply a prediagonalization of the 1D basis (using a simple 1D Hamiltonian) in order to obtain suitable 1D basis functions as linear combinations of the original wavefunctions. This procedure was described in detail in our previous work [25].

Our specific search/selection procedure for constructing the Hamiltonian matrix $H$ in a vibrational calculation, involves the intermediate calculation of a great number of Hamiltonian matrix elements (that are employed to test whether a state should be selected or not), greatly exceeding the final number of elements in $H$. Therefore we need a very fast method for calculation of matrix elements that does not include numerical integrations. For this purpose, prior to each actual vibrational calculation, we compute a number of 2D arrays $P^{i,\alpha_i}_{m_i,n_i} \langle \chi_{m_i}(q_i)|F^{\alpha_i}(q_i)|\chi_{n_i}(q_i)\rangle$, $m_i,n_i = 0,1,2,\ldots,n_{i0}$, corresponding to all vibrational coordinates $q_i$ and each function or operator $F^{\alpha_i}(q_i)$, occurring in either KE or PES expressions, using either Gauss–Hermite, Gauss–Laguerre or Gauss–Legendre numerical integrations [40], where $n_{i0}$ is the number of basis functions employed for the vibrational coordinate $q_i$. All computed $n_{i0} \times n_{i0}$ arrays are stored in computer core memory, ready to use in the subsequent matrix elements calculations. As a result of this and of the separable forms of the KE and PES, each matrix element is obtained as the sum of products of the appropriate $P^{i,\alpha_i}_{m,n}$ values, thus reducing the actual calculation to a number of multiplications and summations and no integrations, which greatly accelerates the calculation of matrix elements.

Our search/selection procedure, serves to select an optimally small however representative active space (AS) of basis states, that are most relevant to the particular vibrational calculation. The aim of our search/selection procedure is the same as the alternative, widely applied in the literature methods for truncation, sequential diagonalization-truncation and energy selected bases techniques [12,13,17–20,41,42], namely to select a small AS from a huge primitive space (PS). The search/selection procedure employed here, described in detail in our work [25], is similar to the artificial intelligence based techniques, developed earlier [43–47]. It is based on the distance $\Delta$ in state space. A search/selection procedure is started from a particular basis (feature) state $|0\rangle$, chosen to be the best zeroth-order representation of the vibrational levels to be calculated (e.g., for calculating the vibrational level structure at the 5th C–O stretch overtone, we choose $|0\rangle = |0,0,6,0,0,0;A_1\rangle$). The algorithm is symmetrically adapted to search and select only such basis states whose symmetry coincides with the symmetry species of the initial state $|0\rangle$. Starting with $|0\rangle$ (as the first state in the AS), the search proceeds to probe first the neighboring ($\Delta = 1$) and next further and further removed ($\Delta = 2,3,\ldots$) basis states $|k\rangle$ in state space, for their coupling strength to $|0\rangle$. Each state that satisfies the criteria for sufficient coupling strength (to be specified below) is selected and consecutively added to the previously selected AS. The probing is done on the basis of an evaluation function $f_k$ that is calculated for each probed state in the search. All selected basis states $|0\rangle$, $|1\rangle$, $|2\rangle$,... are stored in an array in computer core memory together with their $f_k$ values. After $|0\rangle$, the search is conducted in turn on the row of all previously selected states $|1\rangle$, $|2\rangle$, $|3\rangle$,..., leading to the eventual selection of more states. Simultaneously the Hamiltonian matrix is being built, containing the diagonal and nondiagonal matrix elements of all basis states selected so far. The procedure is terminated at the point when, in conducting the search on the last selected state no new states could be selected, according to the criteria of the search.

The three parameters of the search, whose values have to be fixed at the outset, are defined as follows. $R$ is an energy window (around the initial state $|0\rangle$), whose value is usually chosen as 1000 $cm^{-1}$ or larger. Its purpose is to discourage the selection of states that are too far displaced from $|0\rangle$. Another parameter of the search is $f$, the minimum value for the evaluation function $f_k$ of a probed state $|k\rangle$, to be selected ($f$ is usually chosen as $10^{-10}$ or smaller). The initial state of the search $|0\rangle$ takes $f_0 = 1$ and all subsequently selected states obtain smaller and steadily diminishing $f_k$. When a previously selected (parent) state $|n\rangle$ has energy $E_n$ and evaluation function $f_n$, then the evaluation function $f_k$ of a probed state $|k\rangle$ at energy $E_k$ is calculated as: $f_k = f_n \times C_{kn} \times |R/(E_k - E_0)|^2$, where $C_{kn} = |\langle n|H_{vib}|k\rangle/(E_n - E_k)|$ ($C_{kn}$ is set to 1 if it exceeds 1). $C_{kn}$ is compared to the value of $C$, which is the third parameter of the search (normally we set $C = 10^{-9}$ or smaller). When $C_{nk} > C$ and $f_k > f$, the probed state $|k\rangle$ is selected. According to the values chosen for the three parameters $C$, $f$ and $R$, the search/selection procedure will select a varying number of basis states, i.e., include more and more weakly coupled basis states into the selected AS, which will result in enhanced accuracy and convergence in the calculation of the desired molecular vibrational levels.

Our PS for $S_0$ formaldehyde is characterized by following limiting numbers of basis states for the individual coordinates: $n_{0,1} = n_{0,2} = 16$ (CD stretches), $n_{0,3} = 16$ (CO stretch), $n_{0,4} = 38$ (out of plane bend), $n_{0,5} = n_{0,6} = 28$ (DCO bend). This gives a PS dimension of 122,028,032 states, while the states of a particular symmetry species will be ~1/4 of this value. Our AS dimensions range from $N \sim 5000$ to larger than 100000, ensuring a convergence of 0.01 $cm^{-1}$ for the lower excited levels and ~0.1 $cm^{-1}$ for the highest excited ones (at ~17000 $cm^{-1}$). The Hamiltonian matrix $H$ constructed in the course of the search/selection procedure, besides being optimal in size, is also quite sparse, because the algorithm employed automatically discards the matrix elements that are too small according to the criteria of the search. As a result, the actual number of nonzero Hamiltonian matrix elements never exceeds $\sim 100 \times N$, where $N$ is the dimensionality of the AS and of $H$. The sparsity of the obtained Hamiltonian matrix allows it to be stored in computer memory not as a 2D but as a 1D array, including only the nonzero matrix elements. This storage is both memory efficient as well as greatly accelerating the matrix × vector multiplication, which is the most time-consuming step of the Lanczos iteration.

For the tridiagonalization of $H$ we employ a conventional Lanczos iteration without reorthogonalization [47,48], started again with the vector $|0\rangle$.We diagonalize the obtained tridiagonal Lanczos matrix using the routine *tqli*() from Numerical recipes [40]. This latter routine has been modified to yield the eigenvalues $E_i$ and only first component $C_i$ of each eigenvector $|i\rangle$. Usually we perform $2N$ Lanczos iterations. We have found that this is enough to obtain all the important eingenvalues, whose $|C_i|$ values are substantial. We do not remove the spurious eigenvalues, because we only need selected eigenvalues, that converge well and can be easily identified by having the largest overlaps $|C_i|$ with $|0\rangle$. In general, in a vibrational calculation we not only obtain converged eigenvalues $E_i$ and coefficients $C_i$ for all levels in the energetic vicinity of the initial level $|0\rangle$, but also for all the levels at lower energies.

We note, that an alternative basis set filtering procedure using the Lanczos algorithm was employed by Callegari et al. [49] to study the IVR characteristics at CH overtone states in larger molecules like pyrrole and 1,2,3-triazine.

Provided that $|0\rangle$ is the only "bright" basis state (i.e., carrying oscillator strength) in the spectral range of interest, the spectral distribution $C_i(E_i)^2$ represents the absorption spectrum. The characteristic features of this spectrum (width of the spectral distribution, density of spectral lines) are indicative of the extent of vibrational mixing and vibrational fragmentation around $|0\rangle$. The dilution factor $\sigma$ [37] is a good measure of the vibrational fragmentation around $|0\rangle$ and is given by the expression: $\sigma = \sum_k |C_k|^4$ [36]. In fact, $N_{eff} = \sigma^{-1}$ denotes the average number of vibrational eigenstates that are effectively intermixed with (coupled to) the feature (or "bright") state $|0\rangle$, i.e., it represents the extent of vibrational mixing around $|0\rangle$. Another monitor of the extent of vibrational fragmentation around $|0\rangle$ could be the magnitude of the observed local (effective) vibrational level density $\rho_{eff}$, because it includes only those eigenstates, that have substantial $|C_i|$ values and hence substantial vibrational mixing with $|0\rangle$.

## Vibrational calculations

We have calculated the frequencies of most $D_2CO$ vibrational levels in the lower $E_v$ range, up to $E_v \sim 4500$ $cm^{-1}$. These results were converged to better than 0.01 $cm^{-1}$. As in our recent work on $H_2CO$ [25], we have performed careful convergence tests, by varying the values of the search parameters, that resulted in including more weakly coupled basis states into the selected AS. Table 2a illustrates the convergence of the calculated frequency $2\nu_5$ (first overtone of the CD stertch) with increasing active space dimension $N$. Thus we have established, that when using the parameter values $R = 1500$ $cm^{-1}$ and $C = f = 10^{-12}$, our calculated results for these lower excited vibrational levels were correct to 0.01 $cm^{-1}$. In the lower $E_v$ range considered here, each search performed with the above parameter values, selected about $N \sim 5000$–10000 states.

In this energy range the vibrational level structure is quite sparse and assignments do not present a serious problem. Some of these frequencies have been calculated before by other authors [26]. As pointed out above, at present there exists very limited

**Table 1**
Calculated fundamental, overtone and combinational vibrational level frequencies[in $cm^{-1}$] in the lower range of vibrational excitation energies (up to ~4500 $cm^{-1}$) of $S_0$ $D_2CO$, using the MLT quartic PES. Also given for comparison are the existing experimentally measured frequencies as well as calculated values by MLT themselves, using their own PES.

| State | Our calculation | Experiment | Calculated by MLT [26] |
|---|---|---|---|
| $\nu_4(B_1)$ | 941.51 | 938.04 [28] | 939.7 |
| $\nu_6(B_2)$ | 987.60 | 989.25 [28] | 990.3 |
| $\nu_3(A_1)$ | 1107.66 | 1105.7 [2] | 1105.7 |
| $\nu_2(A_1)$ | 1701.79 | 1701.6 [2] | 1702.6 |
| $2\nu_4(A_1)$ | 1872.83 | 1870.47 [27] | 1871.3 |
| $\nu_4 + \nu_6(A_2)$ | 1936.22 | 1930.03 [27] | 1932.7 |
| $2\nu_6(A_1)$ | 1979.26 | 1977.87 [27] | 1976.8 |
| $\nu_3 + \nu_4(B_1)$ | 2049.64 | 2038.91 [27] | 2045.4 |
| $\nu_3 + \nu_6(B_2)$ | 2080.18 | 2072.67 [27] | 2078.9 |
| $\nu_1(A_1)$ | 2061.84 | 2054.69 [27] | 2063.3 |
| $\nu_5(B_2)$ | 2159.52 | 2162.92 [27] | 2157.8 |
| $\nu_2 + \nu_4(B_1)$ | 2637.31 | 2634.7 [29] | 2635.6 |
| $2\nu_3(A_1)$ | 2215.89 | 2201.73 [27] | 2211.3 |
| $\nu_2 + \nu_6(B_2)$ | 2688.25 | 2685.7 [29] | 2687.0 |
| $\nu_2 + \nu_3(A_1)$ | 2806.70 | | 2805.1 |
| $2\nu_2(A_1)$ | 3386.03 | | 3390.2 |
| $3\nu_4(B_1)$ | 2794.86 | 2790.8 [29] | |
| $2\nu_4 + \nu_6(B_2)$ | 2867.98 | 2860.8 [29] | |
| $\nu_4 + 2\nu_6(B_1)$ | 2927.98 | | |
| $3\nu_6(B_2)$ | 2962.86 | | |
| $\nu_3 + 2\nu_4(A_1)$ | 2980.42 | | |
| $\nu_3 + \nu_4 + \nu_6(A_2)$ | 3023.07 | | |
| $\nu_3 + 2\nu_6(A_1)$ | 3052.61 | | |
| $\nu_1 + \nu_4(B_1)$ | 3005.26 | | 2999.1 |
| $\nu_4 + \nu_5(A_2)$ | 3092.67 | | 3085.6 |
| $\nu_1 + \nu_6(B_2)$ | 3053.49 | | 3048.3 |
| $\nu_2 + 2\nu_4(A_1)$ | 3562.66 | | |
| $\nu_5 + \nu_6(A_1)$ | 3148.34 | | 3149.3 |
| $\nu_2 + \nu_4 + \nu_6(A_2)$ | 3626.83 | | |
| $2\nu_3 + \nu_4(B_1)$ | 3158.45 | | |
| $2\nu_3 + \nu_6(B_2)$ | 3173.28 | | |
| $\nu_2 + 2\nu_6(A_1)$ | 3670.32 | | |
| $\nu_1 + \nu_3(A_1)$ | 3156.77 | | 3148.9 |
| $\nu_3 + \nu_5(B_2)$ | 3265.11 | | 3258.5 |
| $\nu_2 + \nu_3 + \nu_4(B_1)$ | 3742.53 | | |
| $\nu_2 + \nu_3 + \nu_6(B_2)$ | 3775.14 | | |
| $3\nu_3(A_1)$ | 3325.20 | | |
| $\nu_1 + \nu_2(A_1)$ | 3758.51 | | 3762.3 |
| $\nu_2 + \nu_5(B_2)$ | 3857.41 | | 3855.9 |
| $2\nu_2 + \nu_4(B_1)$ | 4315.85 | | |
| $4\nu_4(A_1)$ | 3707.96 | | |
| $\nu_2 + 2\nu_3(A_1)$ | 3911.76 | | |
| $2\nu_2 + \nu_6(B_2)$ | 4372.98 | | |
| $3\nu_4 + \nu_6(A_2)$ | 3789.87 | | |
| $2\nu_4 + 2\nu_6(A_1)$ | 3860.01 | | |
| $\nu_4 + 3\nu_6(A_2)$ | 3917.45 | | |
| $2\nu_2 + \nu_3(A_1)$ | 4487.38 | | |
| $\nu_3 + 3\nu_4(B_1)$ | 3901.67 | | |
| $4\nu_6(A_1)$ | 3944.70 | | |
| $\nu_3 + 2\nu_4 + \nu_6(B_2)$ | 3951.41 | | |
| $\nu_1 + 2\nu_4(A_1)$ | 3935.81 | | |
| $\nu_3 + \nu_4 + 2\nu_6(B_1)$ | 3999.71 | | |
| $2\nu_4 + \nu_5(B_2)$ | 4026.73 | | |
| $\nu_3 + 3\nu_6(B_2)$ | 4014.94 | | |
| $\nu_1 + 2\nu_3(A_1)$ | 4250.94 | | |
| $3\nu_2(A_1)$ | 5083.72 | | |
| $\nu_1 + \nu_4 + \nu_6(A_2)$ | 3998.95 | | |
| $\nu_2 + 3\nu_4(B_1)$ | 4478.43 | | |
| $\nu_4 + \nu_5 + \nu_6(B_1)$ | 4089.19 | | |
| $\nu_1 + 2\nu_6(A_1)$ | 4036.73 | | |
| $\nu_5 + 2\nu_6(B_2)$ | 4138.14 | | |
| $2\nu_3 + 2\nu_4(A_1)$ | 4088.58 | | |
| $\nu_2 + 2\nu_4 + \nu_6(B_2)$ | 4552.83 | | |
| $2\nu_3 + \nu_4 + \nu_6(A_2)$ | 4116.14 | | |
| $2\nu_3 + 2\nu_6(A_1)$ | 4137.41 | | |
| $\nu_1 + \nu_3 + \nu_4(B_1)$ | 4099.06 | | |
| $\nu_2 + \nu_4 + 2\nu_6(B_1)$ | 4613.48 | | |
| $\nu_1 + \nu_3 + \nu_6(B_2)$ | 4138.14 | | |
| $2\nu_1(A_1)$ | 4091.90 | | 4098.1 |
| $\nu_2 + 3\nu_6(B_2)$ | 2962.86 | | |
| $\nu_3 + \nu_4 + \nu_5(A_2)$ | 4200.81 | | |
| $\nu_1 + \nu_5(B_2)$ | 4177.73 | | 4170.6 |
| $\nu_2 + \nu_3 + 2\nu_4(A_1)$ | 4667.54 | | |
| $\nu_3 + \nu_5 + \nu_6(A_1)$ | 4250.94 | | |
| $\nu_2 + \nu_3 + \nu_4 + \nu_6(A_2)$ | 4712.62 | | |
| $2\nu_5(A_1)$ | 4296.91 | | 4287.4 |

experimentally measured data for the $D_2CO$ vibrational levels and in addition the frequencies measured by different authors vary by several wavenumbers. All calculated frequencies in this energy range with their assignments, together with the results from previous calculations and experimentally measured data where they exist, are displayed in Table 1.

It is interesting to compare the presently calculated $D_2CO$ frequencies with the results of MLT themselves, using the same PES (also displayed in Table 1). From Table 1 it can be seen, that up to ~3000 $cm^{-1}$, most calculated results by MLT [26] are within 2–3 $cm^{-1}$ of our present (exact) values. The calculated frequencies by MLT above ~3000 $cm^{-1}$ are seen to diverge by up to ~8 $cm^{-1}$ from our results. This disparity is expected to increase at the higher excited levels, but there are no calculated results to compare our results with, in this energy range.

When we compare our calculated frequencies with the available experimentally measured data for $D_2CO$ (not exceeding $E_v \sim 3000\ cm^{-1}$) [2,27–29], we find that the differences range from almost exact coincidence to ~7–8 $cm^{-1}$, and even 11 and 14 $cm^{-1}$ for the $\nu_3 + \nu_4$ and $2\nu_3$ states, respectively. This shows that our calculated frequencies displayed in Table 1 may prove useful for future assignments, when more experimentally measured data at the higher $E_v$ become available.

Next, we have carried out converged calculations on some highly excited vibrational levels of $S_0$ $D_2CO$ up to ~17800 $cm^{-1}$, that are overtones of the $\nu_2$-CO stretch and the $\nu_4$-out-of-plane bend. Both progressions $n\nu_2$ and $n\nu_4$ have been calculated for $D_2CO$ to considerably higher excitation quantum numbers $n$ than for $H_2CO$. For these levels neither previous calculations nor experimentally measured data exist. For each separate calculation, the initial state $|0\rangle$ of the search has been chosen as the appropriate basis overtone state, e.g., for the $17\nu_4$ overtone state we set: $|0\rangle = |0,0,0,17,0,0;B_1\rangle$. For these calculations we have performed careful convergence tests, by varying the parameter values of the search. Two examples for the convergence of vibrational levels in the higher excited energy range are displayed in Table 2b and c. These tests have shown, that the values $R = 1500\ cm^{-1}$, $C = f = 10^{-12}$, are appropriate for these higher excited levels too, but now the selected active spaces were in the range of $N \sim 60000–120000$. Using these parameter values and performing $2N$ iteration steps, all calculated spectral line positions in a window of ~1500 $cm^{-1}$ width around the energy of $|0\rangle$, as well as all intensive lines at energies below $|0\rangle$, were converged to within a few 0.1 $cm^{-1}$. From the obtained reliable spectral picture of all vibrational levels in the considered energy window that are involved in substantial vibrational coupling with the feature state $|0\rangle$, we can count the "effective" vibrational level density. This density was found to be mode specific, as will be demonstrated below. Because of the extensive vibrational fragmentation at such high $E_v$ (as seen from the spectra displayed in Figs. 1 and 2), assignments of the higher overtone states are very difficult and only tentative. The problems encountered with the assignment of the higher excited overtone states are illustrated in Fig. 1, where portions of the calculated spectra in a window of

**Table 2**
Illustration of the convergence of the calculations with increasing active space dimension $N$ (at varying values of the search parameters $R$ and $f$), for three energy levels, located both in the lower and higher excited energy range: (a) $2\nu_5$ at 4296.91 $cm^{-1}$, (b) $13\nu_4$ at 11602.4 $cm^{-1}$, (c) $19\nu_4$ at 16682.4 $cm^{-1}$.

| (a) $2\nu_5$[$cm^{-1}$] | $N$ | $R/f$ |
|---|---|---|
| 4305.298 | 3112 | $1000/10^{-9}$ |
| 4302.755 | 4932 | $1000/10^{-10}$ |
| 4297.844 | 7556 | $1000/10^{-11}$ |
| 4297.538 | 13314 | $1000/10^{-12}$ |
| 4296.935 | 16319 | $1000/10^{-13}$ |
| 4296.912 | 18889 | $1500/10^{-12}$ |
| 4296.905 | 23059 | $1500/10^{-13}$ |
| (b) $13\nu_4$[$cm^{-1}$] | $N$ | $R/f$ |
| 11605.35 | 15962 | $1500/10^{-9}$ |
| 11604.80 | 22318 | $1000/10^{-11}$ |
| 11602.83 | 25642 | $1500/10^{-10}$ |
| 11604.41 | 33839 | $1000/10^{-12}$ |
| 11603.75 | 39111 | $1500/10^{-11}$ |
| 11602.44 | 56603 | $1500/10^{-12}$ |
| (c) $19\nu_4$[$cm^{-1}$] | $N$ | $R/f$ |
| 16382.56 | 19040 | $1000/10^{-9}$ |
| 16383.76 | 30944 | $1000/10^{-10}$ |
| 16381.56 | 69410 | $1000/10^{-12}$ |
| 16382.06 | 130429 | $1500/10^{-12}$ |

200 $cm^{-1}$ width around the expected overtone eigenenergy are displayed, for the six highest excited $n\nu_4$ overtone states. The lines assigned to the relevant overtone states have been indicated by an arrow in the figures. It is readily seen that while at the lower overtone states $11\nu_4$, $12\nu_4$ and $13\nu_4$ the assignment is straightforward, at the higher excited overtones $15\nu_4$, $17\nu_4$ and $19\nu_4$ there is considerable congestion of spectral lines and the assignment can only be tentative. The assigned frequencies, resulting from our calculations on the $n\nu_2$ and $n\nu_4$ overtones are summarized in Table 3. Calculated dilution factors $\sigma$ and vibrational fragmentation $N_{eff} = \sigma^{-1}$ of the overtone levels are also displayed in Table 3, because they are realistic monitors of the vibrational fragmentation and IVR.

The progression $n\nu_2$ in $D_2CO$ is seen to behave similarly to that in $H_2CO$ (the fundamental is close in frequency for both molecules), as regards the dependence of the dilution factor $\sigma$ on $n$ (and $E_v$), (c.f. Table 4, [25]). On the other hand, in $D_2CO$ the dilution factor $\sigma$ of the $n\nu_4$ progression has a different behavior with $n$ (and $E_v$) as compared to $H_2CO$ (cf. Table 4, [25]) (in $D_2CO$ the fundamental $\nu_4$ is about 20% lower in frequency, than in $H_2CO$). Namely, our conclusion from the results displayed in Table 4 [25] was, that the vibrational fragmentation around $n\nu_4$ in $H_2CO$ is comparatively low (and lower than that for $n\nu_2$) i.e., this mode preserves quite good isolation from the remaining molecular vibrations, as seen from the rather large values of the dilution factor $\sigma$, persisting up to rather high excitation levels and energies. On the contrary, it is easily seen from Table 3 of the present work, that in $D_2CO$ the $n\nu_4$ levels have substantially smaller $\sigma$ values than in $H_2CO$ (at comparable $n$ values), which is an indication of greater vibrational fragmentation. It is also seen from Table 3 that the fragmentation at the $n\nu_4$ overtones exceeds substantially that at the $n\nu_2$ progression, i.e. the behavior of the higher excited overtones of $\nu_2$ and $\nu_4$ is inverted in $D_2CO$ as compared to $H_2CO$.

In Fig. 2 we have illustrated the spectral structure obtained from our calculations, for three $n\nu_4$ overtone levels, corresponding to the highest overtone numbers, $n$ = 15, 17 and 19, calculated in this work. For each case, both the entire calculated spectrum, as well as the fine spectral distribution in a window of 50 $cm^{-1}$ around the relevant overtone frequency are displayed in separate pictures. From these latter spectral images, the relevant effective vibrational density $\rho_{eff}$ can be counted. Next, we have compared this spectrally obtained density with the expected total level den-

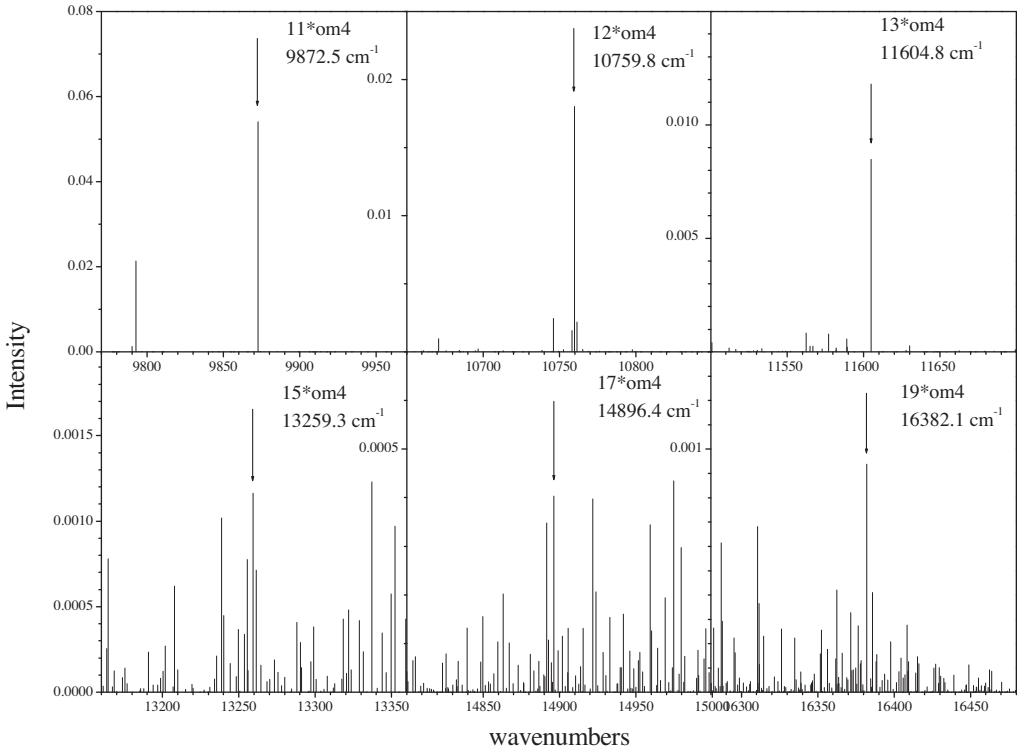


**Fig. 1.** Calculated spectral structures in a window of 200 $cm^{-1}$ around each one of the six higher $n\nu_4$ overtone states, illustrating the assignment problems. The arrow indicates the peak assigned to the relevant overtone state. Intensity=$|C_i|^2$.

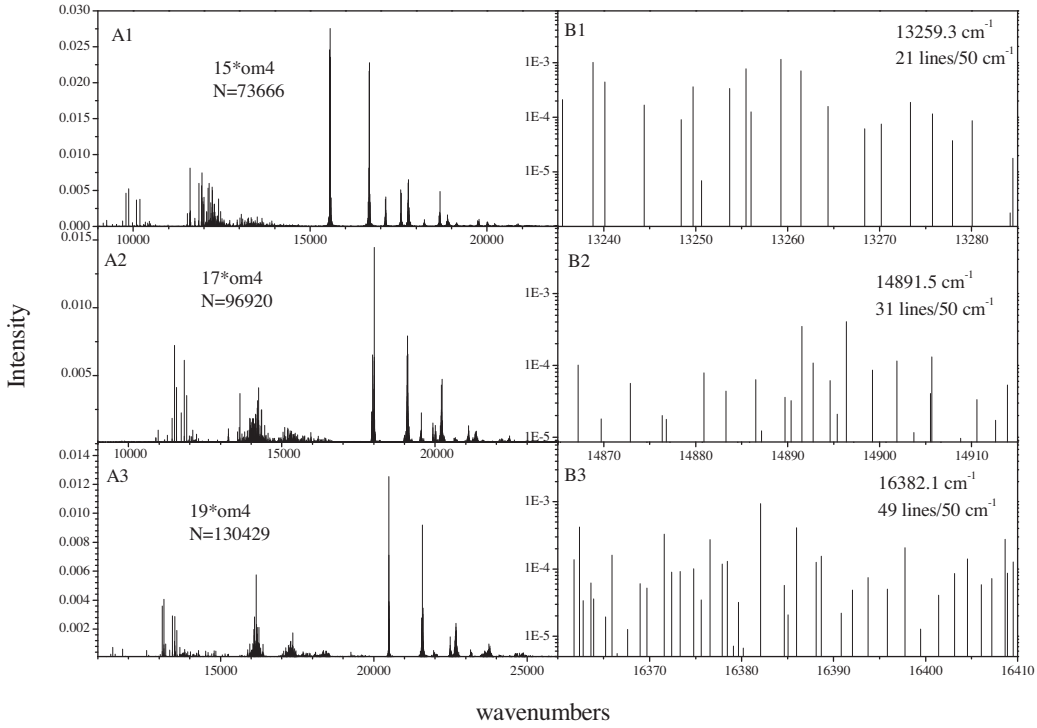


**Fig. 2.** Full calculated spectra (A1, A2, A3) and corresponding spectral sections in a 50 $cm^{-1}$ window around the assigned overtone frequency (B1, B2, B3), for the three highest overtones $15\nu_4$, $17\nu_4$ and $19\nu_4$, respectively, calculated in this work. $N$ is the size of the selected active space. Intensity=$|C_i|^2$.

**Table 3**
Calculated vibrational levels [in $cm^{-1}$] of the higher excited overtone frequencies of the $\nu_2$(C–O stretch) and $\nu_4$ (out-of-plane bend) modes in $S_0$ $D_2CO$; $\sigma$ is the dilution factor and $N_{eff} = 1/\sigma$ the effective number of basis states substantially mixed with the initial state $|0\rangle$; $\rho_{eff}$ is the effectively mixed vibrational level density, counted from the spectra displayed in Fig. 2 (B1,B2,B3) and Fig. 3 (B1,B2,B3), while $\rho_{A1}$ and $\rho_{B1}$ are the estimated total level densities (anharmonic level count) of $A_1$ and $B_1$ symmetry respectively.

| State | Frequency | $\sigma$ | $N_{eff}$ | $\rho_{eff}/\rho_{B1}$ |
|---|---|---|---|---|
| $5\nu_4$ | 4612.3 | 0.24 | 4.2 | |
| $6\nu_4$ | 5508.6 | 0.17 | 5.9 | |
| $7\nu_4$ | 6396.6 | 0.10 | 10.0 | |
| $8\nu_4$ | 7276.5 | 0.065 | 15.4 | |
| $9\nu_4$ | 8149.2 | 0.038 | 26.3 | |
| $10\nu_4$ | 9014.9 | 0.023 | 43.5 | |
| $11\nu_4$ | 9871.8 | 0.015 | 66.7 | |
| $12\nu_4$ | 10757.9 | 0.0069 | 144.9 | |
| $13\nu_4$ | 11602.4 | 0.0064 | 156.2 | |
| $15\nu_4$ | 13300.1 | 0.0051 | 196.1 | 0.66 |
| $17\nu_4$ | 14995.7 | 0.0013 | 769.2 | 0.54 |
| $19\nu_4$ | 16682.4 | 0.00083 | 1204.8 | 0.56 |

| State | Frequency | $\sigma$ | $N_{eff}$ | $\rho_{eff}/\rho_{A1}$ |
|---|---|---|---|---|
| $3\nu_2$ | 5052.3 | 0.31 | 3.2 | |
| $4\nu_2$ | 6700.4 | 0.19 | 5.3 | |
| $5\nu_2$ | 8330.2 | 0.10 | 10.0 | |
| $6\nu_2$ | 9943.1 | 0.058 | 17.2 | |
| $7\nu_2$ | 11541.5 | 0.046 | 21.7 | |
| $8\nu_2$ | 13128.3 | 0.039 | 25.6 | |
| $9\nu_2$ | 14704.4 | 0.025 | 40.0 | 0.56 |
| $10\nu_2$ | 16262.5 | 0.013 | 76.9 | 0.42 |
| $11\nu_2$ | 17806.3 | 0.011 | 90.9 | 0.26 |

sity (of suitable symmetry type, $\rho_{B1}$), computed using a conventional anharmonic vibrational level count. For the $15\nu_4$ overtone at $E_v = 13300$ $cm^{-1}$, we obtained from the spectrum (see Fig. 2B1) an effective level density of $\rho_{eff} = 0.42$ $l/cm^{-1}$. The anharmonic level count at this $E_v$ yields a total $B_1$ density of $\rho_{B1} = 0.64$ $l/cm^{-1}$, i.e. $\rho_{eff}/\rho_{B1} = 0.66$. Next, considering the $17\nu_4$ overtone at $E_v = 14995$ $cm^{-1}$ (Fig. 2A2 and B2), we counted from Fig. 2B2 the effective level density to be $\rho_{eff} \sim 0.62$ $l/cm^{-1}$, while the anharmonic level count at this $E_v$ yields a total $B_1$ density of $\rho_{B1} \sim 1.14$ $l/cm^{-1}$, i.e. $\rho_{eff}/\rho_{B1} = 0.54$. Finally, considering the $19\nu_4$ overtone at $E_v = 16682$ $cm^{-1}$ (Fig. 2A3 and B3), we find from Fig. 2B3 that the effective level density is $\rho_{eff} \sim 0.98$ $l/cm^{-1}$, while the anharmonic level count at this $E_v$ yields a total $B_1$ density of $\rho_{B1} \sim 1.75$ $l/cm^{-1}$, i.e. in this case the portion of the spectrally measured effective level density is about 56% ($\rho_{eff}/\rho_{B1} = 0.56$) of the entire available $B_1$ vibrational level density.

Next, in Fig. 3 we have illustrated the spectral structures obtained from our calculations on the three $n\nu_2$ overtone levels, corresponding to the highest overtone numbers, $n = 9$, 10 and 11, accessed in this work. For each case, both the entire calculated spectrum (Fig. 3A1–A3), as well as the fine spectral distribution in a window of 50 $cm^{-1}$ around the relevant overtone frequency (Fig. 3B1–B3), are displayed in separate pictures. As above, the effective vibrational density $\rho_{eff}$ was counted from these latter images. For overtone state $9\nu_2$ at 14704 $cm^{-1}$, the effective level density counted from Fig. 3, B1 was $\rho_{eff} \sim 0.56$ $l/cm^{-1}$. This amounted to 56% from the available anharmonically counted $A_1$ vibrational density of 1 $l/cm^{-1}$. Next, for the $10\nu_2$ state at 16262 $cm^{-1}$, the effective level density counted from Fig. 3B2 was $\rho_{eff} \sim 0.70$ $l/cm^{-1}$ and this amounted to 42% from the available $A_1$ vibrational level density of $\rho_{A1} \sim 1.65$ $l/cm^{-1}$. For the $11\nu_2$ state at 17806 $cm^{-1}$ (Fig. 3B3), the effective spectrally obtained density was $\rho_{eff} \sim 0.66$ $l/cm^{-1}$, which amounted to only 26% from the available anharmonically counted $A_1$ vibrational density of $\rho_{A1} \sim 2.5$ $l/cm^{-1}$.

The obtained ratios $\rho_{eff}/\rho_{B1}$ for the $15\nu_4$, $17\nu_4$ and $19\nu_4$ overtones as well as the $\rho_{eff}/\rho_{A1}$ ratios for the $9\nu_2$, $10\nu_2$ and $11\nu_2$ overtones are displayed in the last column of Table 3. It is readily seen that these data confirm the conclusions drawn from the dilution factors, namely that there is strong fragmentation at the higher

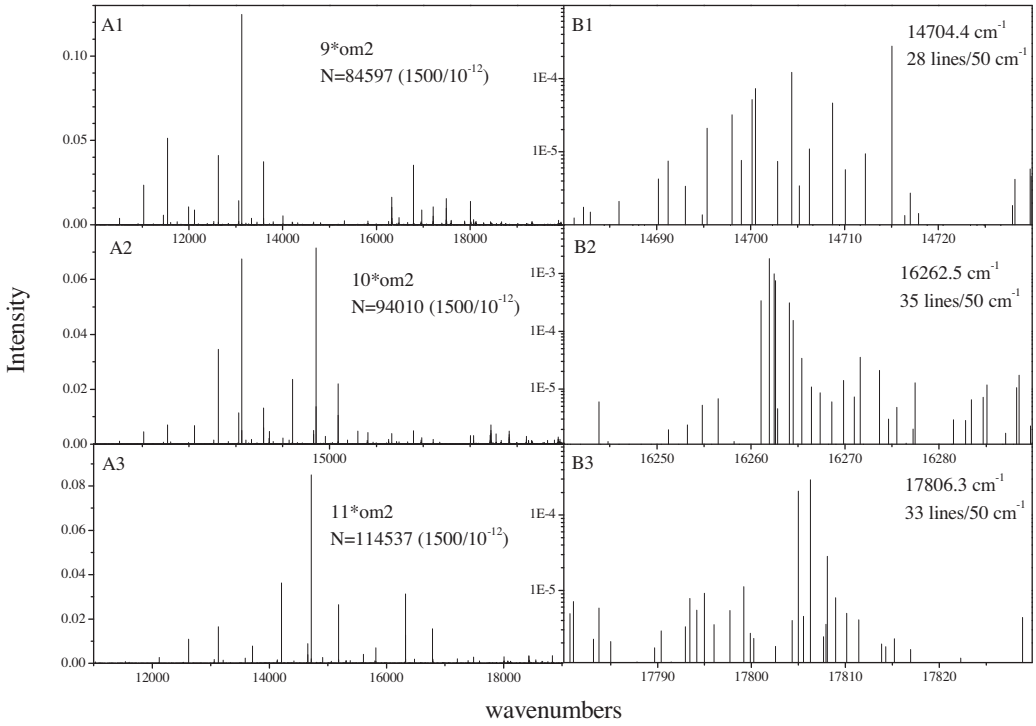


**Fig. 3.** Full calculated spectra (A1, A2, A3) and corresponding spectral sections in a 50 $cm^{-1}$ window around the assigned overtone frequency (B1, B2, B3), for the three highest overtones $9\nu_2$, $10\nu_2$ and $11\nu_2$, respectively, calculated in this work. $N$ is the size of the selected active space. Intensity=$|C_i|^2$.

$n\nu_4$ overtones (about half the available vibrational density is involved in the vibrational mixing), while there is an increasing isolation of the $n\nu_2$ states with $n$ (a steadily decreasing portion of the available vibrational density is involved in the vibrational mixing).

How could these observations be extrapolated to the higher excited and chemically interesting vibrational levels of $S_0$ $D_2CO$ at ~28000 $cm^{-1}$, that were studied by Polik et al. [30]? No definite conclusions can be drawn about the photophysical and photochemical behavior of those levels from our present results, yet it may be possible to trace some tendencies. In general we have found beyond any doubt, that vibrational mixing in $S_0$ $D_2CO$ is very far from being complete up to vibrational excitation energies of ~17000 $cm^{-1}$. This is especially true for the progression in the $\nu_2$ mode, that displays increasing isolation with the overtone number n, but also for the levels from the progression of the $\nu_4$ mode, where the portion of the effective (vibrationally intermixed) level density is about half the available vibrational density and this portion does not essentially grow with the overtone number n (Table 3). Thus it is logical to expect that the restricted character of IVR might persist up to the chemically interesting levels at $E_v \sim 28300$ $cm^{-1}$, accessed by Polik et al. [30]. Furthermore Waite et al. [50] have inferred theoretically that incomplete mixing of the out-of-plane mode with the in-plane modes and the in-plane reaction coordinate may cause the reaction rates of individual levels to vary by at least two orders of magnitude. Indeed, the authors [30] observed experimentally wide distributions (of about two orders of magnitude) in both the dissociation widths and nonradiative coupling matrix elements of closely located $S_0$ vibrational levels at $E_v \sim 28300$ $cm^{-1}$, demonstrating that each level exhibits specific chemical and photophysical behavior related to its individual vibrational characater.

## Conclusions

In the present work we have applied on $S_0$ $D_2CO$ our recently developed variational procedure for calculating highly excited vibrational energy levels in formaldehyde, that is based on a specific search/selection procedure for contraction of the huge primitive basis space and a Lanczos iteration procedure for extraction of the required eigenvalue and eigenvector information. We employed the exact expression of the molecular vibrational kinetic energy operator and the exact ab initio MLT quartic potential field. Using our vibrational procedure, we have carried out converged high precision calculations and assignments of a large number of $S_0$ $D_2CO$ vibrational levels up to excess vibrational energy of about 4500 $cm^{-1}$. We have compared the results of these calculations with the few existing experimentally measured frequencies as well as with the calculated results by other authors using the same PES. The calculated frequencies in the present work may prove useful for future assignments of experimentally measured frequencies, when such data for $D_2CO$ become available. Next, using our vibrational procedure, we have performed large scale calculations on a number of highly excited states (up to ~17800 $cm^{-1}$), belonging to the $n\nu_2$ and $n\nu_4$ overtone progressions. Besides demonstrating the possibilities of our method, it was our aim to investigate the extent of vibrational mixing and IVR at very high $E_v$ in $S_0$ $D_2CO$, where some signs of the interesting photophysical and photochemical behavior of this molecule might start to appear. For that purpose we have analyzed dilution factors for all calculated levels, indicating the extent of vibrational fragmentation and IVR at the basis states of interest. In addition, from the calculated fine spectral structures we have been able to determine the magnitude of the vibrationally coupled (effective) level density. The ratio of the effective density to the entire available vibrational density (of appropriate symmetry), was used as another monitor of the vibrational mixing and IVR behavior at the studied states. In general, we have found that up to $E_v \sim 17000$ $cm^{-1}$ IVR is not complete neither tends to completion and there exists well expressed mode specificity. Furthermore, a definite distinction was found in the local mode and IVR behavior of the $n\nu_2$ and $n\nu_4$ progressions with the overtone number $n$ in $D_2CO$, as well as between the two molecules $H_2CO$ and $D_2CO$.

## Acknowledgement

This research was supported by the National Research and Engineering Council of Canada and grant BG051PO001/3.3-05 from the Bulgarian Ministry of Education and Science.

## References

[1] D.C. Moule, A.D. Walsh, Chem. Rev. 75 (1975) 67.
[2] D.J. Clouthier, D.A. Ramsay, Annu. Rev. Phys. Chem. 34 (1983) 31.
[3] J.L. Hardwick, S.M. Till, J. Chem. Phys. 70 (1979) 2340.
[4] L.R. Brown, R.H. Hunt, A.S. Pine, J. Mol. Spectrosc. 75 (1979) 406.
[5] D.E. Reisner, R.W. Field, J.L. Kinsey, H.L. Dai, J. Chem. Phys. 80 (1984) 5968.
[6] R.J. Bouwens, J.A. Hammerschmidt, M.M. Grzeskowiak, T.A. Stegink, P.M. Yorba, W.F. Polik, J. Chem. Phys. 104 (1996) 460.
[7] D. Luckhaus, M.J. Coffey, M.D. Fritz, F.F. Crim, J. Chem. Phys. 104 (1996) 3472.
[8] N.C. Handy, Mol. Phys. 61 (1987) 207.
[9] H. Romanowski, J.M. Bowman, L.B. Harding, J. Chem. Phys. 82 (1985) 4156.
[10] M. Aoyagi, S.K. Gray, M.J. Davis, J. Opt. Soc. Am. B7 (1990) 1859.
[11] M. Aoyagi, S.K. Gray, J. Chem. Phys. 94 (1991) 195.
[12] M.J. Bramley, T. Carrington, J. Chem. Phys. 99 (1993) 8519.
[13] S. Carter, N. Pinnavaia, N.C. Handy, Chem. Phys. Lett. 240 (1995) 400.
[14] S. Carter, N.C. Handy, J. Mol. Spectrosc. 179 (1996) 65.
[15] N.M. Poulin, M.J. Bramley, T. Carrington Jr., H.G. Kjaergaard, R. Henry, J. Chem. Phys. 104 (1996) 7807.
[16] D.C. Burleigh, A.B. McCoy, E.L. Sibert III, J. Chem. Phys. 104 (1996) 480.
[17] D. Luckhaus, J. Chem. Phys. 113 (2000) 1329.
[18] F. Ribeiro, C. Iung, C. Leforestier, Chem. Phys. Lett. 362 (2002) 199.
[19] M. Mladenovic, Spectrochim. Acta A58 (2002) 809.
[20] H.-S. Lee, J.C. Light, J. Chem. Phys. 120 (2004) 4626.
[21] R. Bernal, R. Lemus, J. Mol. Spectrosc. 235 (2006) 218.
[22] M. Sanchez-Castellanos, R. Lemus, J. Mol. Spectrosc. 266 (2011) 1.
[23] A. Yachmenev, S.N. Yurchenko, P. Jensen, W. Thiel, J. Chem. Phys. 134 (2011) 244307.
[24] S. Rashev, D.C. Moule, Cent. Eur. J. Chem. 9 (2011) 549–556.
[25] S. Rashev, D.C. Moule, Spectrochim. Acta A: Mol. Biomol. Spectrosc. 87 (2012) 286–292.
[26] J.M.L. Martin, T.J. Lee, P.R. Taylor, J. Mol. Spectrosc. 160 (1993) 105.
[27] J. Lohilalti, O.N. Uleinikov, E.S. Bekhtereva, S. Alanko, R. Antilla, J. Mol. Struct. 780–781 (2006) 182.
[28] A. Perrin, J.-M. Flaud, A. Predoi-Cross, M. Winnewisser, B.P. Winnewisser, G. Mellau, M. Lock, J. Mol. Spectrosc. 187 (1998) 61.
[29] G.D. Martin, T.P. Chassee, T.O. Friday, W.H.Polik, Dispersed Fluorescence Spectroscopy of $D_2CO$. Available from: http://www.chem.hope.edu/≃polik/poster/d2co96.htm
[30] W.F. Polik, D.R. Guyer, C.B. Moore, J. Chem. Phys. 92 (1990) 3453.
[31] E.S. Yeung, C.B. Moore, J. Chem. Phys. 58 (1973) 3988.
[32] C.B. Moore, J.C. Weisshaar, Annu. Rev. Phys. Chem. 43 (1983) 525.
[33] Y.S. Choi, C.B. Moore, J. Chem. Phys. 94 (1991) 5414.
[34] P. Chowdary, M. Gruebele, J. Chem. Phys. 130 (2009) 024305.
[35] P. Chowdary, M. Gruebele, J. Chem. Phys. 130 (2009) 134310.
[36] E.L. Sibert III, M. Gruebele, J. Chem. Phys. 124 (2006) 024317.
[37] G.M. Stewart, J.D. McDonald, J. Chem. Phys. 78 (1983) 3907.
[38] G. Pasin, F. Gatti, C. Iung, H.-D. Meyer, J. Chem. Phys. 124 (2006) 194304.
[39] G. Pasin, C. Iung, F. Gatti, H.-D. Meyer, J. Chem. Phys. 126 (2007) 024302.
[40] W.H. Press, B.P. Flannery, S.A. Teukolsky, W.T. Vetterling, Numerical Recipes in C, Cambridge University Press, Cambridge, 1988.
[41] J.M. Bowman, T. Carrington, H.-D. Meyer, J. Mol. Phys. 106 (2008) 2145.
[42] J.C. Light, T. Carrington, Adv. Chem. Phys. 114 (2000) 265.
[43] S.M. Lederman, R.A. Marcus, J. Chem. Phys. 88 (1988) 6312.
[44] Y. Zhang, R.A. Marcus, J. Chem. Phys. 96 (1992) 6065.
[45] J. Chang, R.E. Wyatt, J. Chem. Phys. 85 (1986) 1826.
[46] J. Chang, N. Moiseyev, R.E. Wyatt, J. Chem. Phys. 84 (1986) 4997.
[47] R.E. Wyatt, Adv. Chem. Phys. 73 (1989) 231.
[48] J.K. Cullum, R.A. Willowghby, "Lanczos Algorithms for Large Symmetric Eigenvalue Computations", vols. I and II (Birkhauser, Boston, 1985).
[49] A. Callegari, R. Pearman, S. Choi, P. Engels, H. Srivastava, M. Gruebele, K.K. Lehmann, G. Scholes, J. Mol. Phys. 101 (2003) 551.
[50] B.A. Waite, S.K. Gray, W.H. Miller, J. Chem. Phys. 78 (1983) 259.